Orthorhombic ABC semiconductors as antiferroelectrics

Joseph W. Bennett*, Kevin F. Garrity*, Karin M. Rabe and David Vanderbilt
Department of Physics and Astronomy
Rutgers University, Piscataway, NJ 08854 and
*These authors contributed equally to the present work.
(Dated: October 29, 2012)

We use a first-principles rational-design approach to identify a previously-unrecognized class of antiferroelectric materials in the $Pnma$ MgSrSi structure type. The MgSrSi structure type can be described in terms of antipolar distortions of the nonpolar $P6_3/mmc$ ZrBeSi structure type, and we find many members of this structure type are close in energy to the related polar $P6_3mc$ LiGaGe structure type, which includes many members we predict to be ferroelectric. We highlight known ABC combinations in which this energy difference is comparable to the antiferroelectric-ferroelectric switching barrier of PbZrO$_3$. We calculate structural parameters and relative energies for all three structure types, both for reported and as-yet hypothetical representatives of this class. Our results provide guidance for the experimental realization and further investigation of high-performance materials suitable for practical applications.

There has been great progress in the use of first-principles methods in the design and discovery of new functional materials, most notably for the rapid evaluation and screening of a large number of known and as-yet hypothetical compounds in a target family already known to contain compounds exhibiting the desired functional behavior[1–4]. A greater challenge is to develop ways to identify new functional materials in families in which the desired behavior has been previously unrecognized. In recent work, we used a combined crystallographic database/first-principles approach [5] to identify semiconducting members of the family of compounds in the LiGaGe structure type as a previously unrecognized class of ferroelectrics, characterized by spontaneous polarizations and barriers to polarization switching comparable to the much-studied ferroelectric ABO_3 perovskite oxides [5, 6]. Here, we apply this approach to identify a previously unrecognized class of antiferroelectrics, opening the way to increased recognition and application of antiferroelectrics as functional materials.

An antiferroelectric [7, 8] is like a ferroelectric in that its structure is obtained through distortion of a nonpolar high-symmetry reference phase; for ferroelectrics, the distortion is polar, while for antiferroelectrics it is nonpolar. However, not all nonpolar phases thus obtained are antiferroelectric: in addition, there must be an alternative low-energy ferroelectric phase obtained by a polar distortion of the same high-symmetry reference structure, and an applied electric field must induce a first-order transition from the antiferroelectric phase to this ferroelectric phase, producing a characteristic P-E double-hysteresis loop [9, 10]. This behavior in applied electric field is the origin of the functional properties of antiferroelectrics. For systems in which there is a difference in lattice parameters between the AFE and FE phases, the electric-field-induced transition produces a large nonlinear strain response, useful for transducer applications [11]. The en-tropy change between the two phases similarly can produce a high effective electrocaloric response, useful for solid-state cooling [12]. Finally, the shape of the P-E hysteresis loop allows storage of electrical energy of sufficient magnitude to attract interest for energy storage applications [13, 14].

Most of the research on antiferroelectric oxides has focused on two classes of materials, both with rather complex structures. The $Pbam$ structure of the prototypical perovskite antiferroelectric PbZrO$_3$[9] is obtained through a cell-quadrupling antipolar Pb displacement mode combined with four additional modes that further double the unit cell [15]; the $Pbcm$ structure of the antiferroelectric phases of NaNbO$_3$ and AgNbO$_3$ are similarly complex [16]. Chemical substitution into the end-point compounds allows tuning of the critical temperature, the critical field, the electric-field induced strain and polarization, and other functional properties [14, 17]. Chemical substitution is also seen to induce transitions to a distinct tetragonal antiferroelectric phase, for example in Pb$_{1-x}$Sr$_x$(Zr$_{1-y}$Ti$_y$)O$_3$ [11], and to related ferroelectric phases, for example in PbZr$_{1-x}$Ti$_x$O$_3$, also obtained as distortions of the ideal perovskite structure.

Evidence is beginning to emerge that antiferroelectricity in inorganic materials extends far beyond the systems which have been the focus of the literature to date. In particular, recent observations of orthorhombic $Pnma$ Sm-doped BiFeO$_3$ [18] and thin-film BiCrO$_3$ [19] show the double hysteresis loops characteristic of antiferroelectricity. This suggests that many additional nonpolar phases should be considered as candidates for previously-unrecognized antiferroelectricity. Our strategy to search for new antiferroelectric materials is to identify a class of materials with a structure type that is obtained from an antipolar distortion of a high-symmetry reference structure which is also related through a polar distortion to a structure type of known ferroelectrics. By screen-

ing a large number of both reported and hypothetical compounds, we can find compositions that are insulating and locally stable both in the antiferroelectric structure and in the related ferroelectric structure; of these, the compounds for which the antiferroelectric structure is slightly lower in energy than the ferroelectric structure are promising candidates for new antiferroelectrics for targeted experimental investigation. Through this search, we expect to find new AFE structure types which are significantly simpler than the *Pbam* structure, even perhaps including realizations of the two-sublattice Kittel model [10] and $q=0$ antiferroelectrics [20]. For technological applications, new materials offer the possibility of better performance via reduced hysteresis, larger changes at the electric-field-induced transition, operation at higher or lower temperatures, better integration with other materials based on structural or chemical compatibility, elimination of toxic elements, and/or a band gap suitable for photoactive applications.

ABC compounds in the *Pnma* MgSrSi structure type [21] (previously referred to as the anti-PbCl$_2$ structure type [22]) are a promising target class. The MgSrSi structure, shown in Fig. 1, is obtained by a nonpolar distortion of the high-symmetry $P6_3/mmc$ ZrBeSi structure. The distortion can be decomposed into two modes: an M_2^- mode (antipolar displacements of *ABC* along c, and antipolar displacements of A along b) that breaks the $P6_3/mmc$ symmetry to *Pnma*, followed by a Γ_5^+ mode (shifting of *BC* layers along b) that does not break any additional symmetry. A polar distortion specified by a Γ_2^- mode relates the high-symmetry $P6_3/mmc$ structure to the LiGaGe-type $P6_3mc$ ferroelectric compounds identified previously [5]; in addition to being insulating, these compounds can have spontaneous polarization comparable to that of BaTiO$_3$. However, little has been reported about the band structure of MgSrSi-type compounds or about their response to applied electric fields [23, 24].

In this paper, we use first-principles methods to establish a new class of antiferroelectrics in the MgSrSi structure type and to identify promising candidate materials for further investigation. Specifically, we compute the structural parameters, nonpolar distortions, band gaps, and AFE-FE energy differences for a search set comprising 37 reported and 33 as-yet-hypothetical *ABC* compounds in the MgSrSi structure type. We identify 11 combinations for which both the FE and AFE phases are insulating and have an energy difference below 0.2 eV. For all insulating combinations studied, we find that the band gaps are in the semiconducting range; the lower band gaps could be useful for photoactive applications [25–27]. These candidate antiferroelectrics offer promise for experimental investigation and for the future development of new high-performance materials for practical applications.

First principles computations were performed with the ABINIT package [28]. The local density approximation
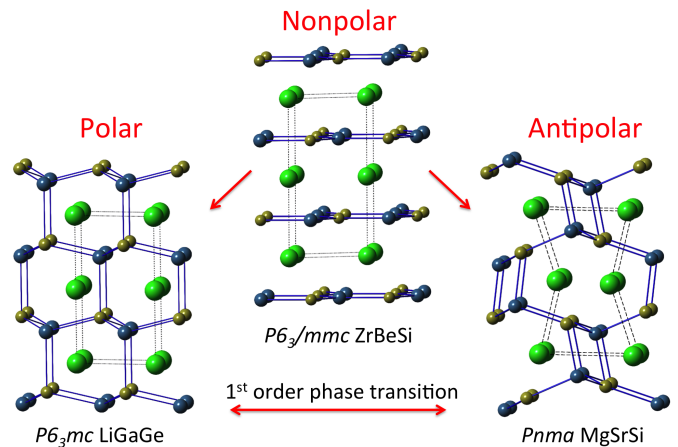

FIG. 1: Left: planar buckling distortions of the polar $P6_3mc$ LiGaGe structure relative to the $P6_3/mmc$ high symmetry ZrBeSi structure type (center), as described in Ref. [5]. Right: antipolar distortions of the *Pnma* MgSrSi structure type relative to the high symmetry ZrBeSi structure type (center), showing antipolar buckling of the planes formed by atoms *BC* at Wyckoff positions $2b$ (dark blue) and $2b'$ (gold) and antipolar displacements of the stuffing atoms A at $2a$ (green).

(LDA) and a 6×6×6 Monkhorst-Pack sampling of the Brillouin zone [29] were used for all calculations, except for the Berry phase polarization [30, 31] calculations, for which an 8×8×8 grid was used. All atoms were represented by norm-conserving, optimized [32], designed nonlocal [33] pseudopotentials, generated with the OPIUM code [34]. All calculations were performed with a plane wave cutoff of 50 Ry. In addition, the QUANTUM ESPRESSO [35] package was used to perform nudged elastic band calculations [36, 37]. WANNIER90 [38] was used to generate maximally localized Wannier functions (MLWF) [39].

Our search set of candidate MgSrSi-type antiferroelectrics consists of *ABC* combinations drawn from the *Inorganic Crystal Structural Database* (ICSD) [40] and two recent high-throughput searches. The ICSD includes 37 previously synthesized *ABC* compounds in the MgSrSi structure type that do not contain an f-block element and which have a total of 8 or 18 valence electrons, which promotes band gap formation. In addition, we included 13 as-yet unsynthesized compounds from the high-throughput study of Zhang *et al.* [3] that are predicted to have the desired *Pnma* structure. Finally, we included 20 compounds from the high-throughput study of Bennett *et al.* [5] that are predicted to be insulating and at least locally stable in the polar LiGaGe structure type, bringing our total search set to 70 compounds. We can classify these combinations into the following groups: I-I-VI (NaKSe), I-II-V (LiCaBi), I-XII-V (NaCdAs), XI-II-V (CuMgP), II-II-IV (SrCaGe), III-X-V (ScNiP), III-XI-IV (ScCuSi), and IV-X-IV (ZrPtSi).

For each *ABC* combination in our search set, we op-

timize the structural parameters for each of the three structural variants $\underline{A}BC$, $A\underline{B}C$, and $AB\underline{C}$, where the underscore indicates the stuffing atom (Fig. 1), for each of our three structure types: MgSrSi ($Pnma$), LiGaGe ($P6_3mc$), and ZrBeSi ($P6_3/mmc$). The computed structural parameters (Supplemental Table 1) generally show good agreement with experimental values, with the underestimate of lattice constants characteristic of LDA calculations, about 1-3 % for a and as large as 3-4 % for c[44]. While most of our calculations agree with previous experimental and theoretical determinations of the ground state structure, there are a few minor discrepancies. We find that NaCdSb prefers the $P6_3mc$ structure by 34 meV/f.u. over the experimentally reported $Pnma$ structure. In addition, we find that KSrBi and RbBaAs prefer the high-symmetry $P6_3/mmc$ structure, in contrast to the results of Zhang et al.[3], which we attribute to minor methodological differences [45].

Our most promising candidate antiferroelectrics, shown in Table I, fulfill the following criteria: a) the ground state is the antipolar $Pnma$ MgSrSi structure type, b) the polar $P6_3mc$ LiGaGe structure type is metastable, and c) both phases are insulating. In Table I we present the energy differences between the $Pnma$ and $P6_3mc$ structures (ΔE), the energy difference between the $P6_3mc$ and $P6_3/mmc$ (ΔE_{SW}), the polarization of the LiGaGe structure, the mode decomposition of the antipolar distortions, and difference in volume between the $P6_3mc$ and $Pnma$ structures. Of this set, seven combinations are known materials, highlighted in boldface in Table I. The calculated band gaps of these materials cover the entire semiconducting range, from 0.04 eV (BaCaSi) to 2.91 eV (NaLiTe), with changes of 0.01 to 0.59 eV upon switching (see Supplemental Tables).

We find eleven insulating compounds with energy differences between the polar and antipolar phases below 0.2 eV/f.u. (see Table I). Of this set, six combinations, namely LiCaBi, LiCaSb, KNaTe, NaLiTe, KNaS, and KNaSe, are known materials. Despite the small energy differences, many of our candidate materials still require a large critical field to stabilize the polar phase. However, the structural versatility of ABC intermetallic compounds should make it experimentally feasible to reduce the critical field of many of these materials via formation of solid solutions of chemically similar compounds with different structures. For instance, we find that LiBeP has an antipolar $Pnma$ ground state, while LiBeAs has a polar $P6_3mc$ ground state. A solid solution of these two materials should result in a material in which it is possible to chemically tune towards the first-order transition between preferred structures, thus reducing the critical field.

In addition to our most promising candidates, in Table II we present data for seven compounds that have a $Pnma$ ground state as well as a stable polar distortion, but for which only one of the two phases is in-

ABC	ΔE_{SW} (meV)	P (C/m^2)	Γ_5^+	M_2^-	ΔE (meV)	ΔV (Å^3)	$\Delta V/V$ (%)
LiBeP	119	0.85	0.26	1.26	18	1.23	3.7
MgLiP	20	0.38	0.41	1.28	230	0.49	1.1
MgLiAs	30	0.39	0.42	1.35	207	0.12	0.2
CaLiSb	7	0.18	0.19	1.17	79	0.09	0.1
CaLiBi	7	0.19	0.20	1.16	80	−0.10	−0.1
NaMgP	102	0.49	0.31	1.43	275	1.88	3.2
NaMgAs	114	0.48	0.34	1.44	232	1.65	2.5
NaMgSb	146	0.43	0.40	1.51	154	0.93	1.2
NaMgBi	127	0.42	0.44	1.51	143	1.14	1.4
KMgSb	41	0.40	0.33	1.77	254	2.17	2.6
KMgBi	73	0.31	0.34	1.78	227	1.65	1.8
NaZnSb	81	0.49	0.18	1.48	42	2.68	4.1
NaLiTe	23	0.20	0.30	1.41	114	0.96	1.4
KNaS	12	0.17	0.32	1.36	149	1.60	2.3
KNaSe	13	0.15	0.33	1.38	131	2.09	2.7
KNaTe	14	0.13	0.38	1.42	96	2.81	2.9
NaAgSe	51	0.65	0.62	1.63	134	0.11	0.2
BaCaSi	11	0.34	0.35	1.62	310	0.37	0.4

TABLE I: Energy difference between $P6_3mc$ and $P6_3/mmc$ phases (ΔE_{SW}), polarization P, amplitude of the microscopic distortions from ZrBeSi to MgSrSi structure types (Γ_5^+ and M_2^-), energy difference between AFE and FE states (ΔE), and change in volume (ΔV), also given as a percentage, for the eighteen compounds in the search set that are insulating in both the antipolar and polar states. Combinations reported as $Pnma$ in the ICSD are shown in boldface. Energies are reported in meV per formula unit. Band gaps are reported in the supplemental material.

ABC	ΔE_{SW} (meV)	P (C/m^2)	Γ_5^+	M_2^-	ΔE (meV)	ΔV (Å^3)	$\Delta V/V$ (%)
MgLiSb	50	—	0.48	1.42	142	1.32	2.2
MgLiBi	41	—	0.52	1.45	126	1.52	2.4
MgCuP	1	0.36	0.42	1.43	174	−0.58	−1.3
NaZnBi	328	—	0.18	1.28	18	2.50	3.6
NaCdAs	199	0.40	0.31	1.44	50	1.54	2.4
SrCaGe	2	0.04	0.27	1.36	186	3.72	4.6
BaCaGe	11	0.26	0.37	1.59	289	1.04	1.1

TABLE II: Same as Table 1, but for compounds in the search set for which either the $Pnma$ state or the $P6_3mc$ state is metallic in our DFT calculation. A dash in the polarization (P) column indicates that the $P6_3mc$ state is metallic.

sulating. This caveat would normally disqualify these compounds as candidate antiferroelectrics, but it is well known that DFT-LDA tends to significantly underestimate band gaps, and can even predict small-gap semiconductors (e.g., Ge) to be metallic [41]. It is possible that these seven compounds could display antiferroelectric behavior, and therefore merit experimental investigation, especially since four are known materials (highlighted in boldface in Table II).
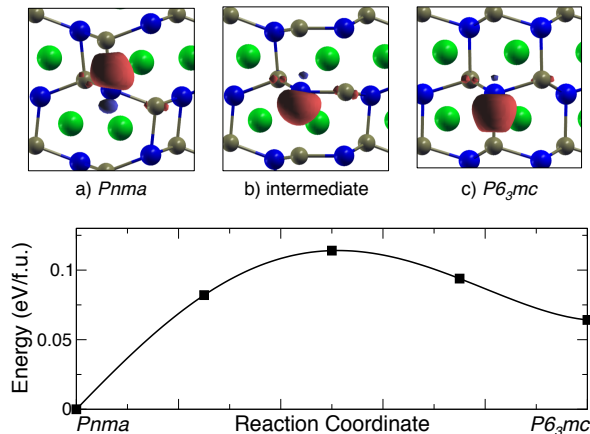
FIG. 2: Minimum-energy path for switching between the non-polar $Pnma$ and polar $P6_3mc$ phases of NaCdAs, as calculated by the NEB method. (a-c): isosurfaces of an inter-planar bonding state (MLWF), which reverses orientation during the switching process. Lower panel: graph of energy vs reaction coordinate, showing that our proposed reaction pathway from $Pnma$ to $P6_3mc$ has a barrier of 0.11 eV. This is in comparison to a path that would have the high-symmetry $P6_3/mmc$ structure as our intermediate, which would be 0.19 eV.

In order to investigate the switching path between the antipolar and polar states, we use nudged elastic band calculations (with the volume fixed to the $Pnma$ cell) to identify the lowest-energy path between the two phases, as shown in Fig. 2. While we expect that the actual experimental switching path will depend on complex kinetic processes like domain nucleation and domain-wall motion, our calculations of homogeneous switching paths provide an estimate of the energy scales involved. For our example of NaCdAs in Fig. 2, we find that the low-energy switching path from $Pnma$ to $P6_3mc$ corresponds primarily to half of the Cd atoms moving from below the As layer to above it, while the Na atoms rearrange to avoid the Cd. For NaCdAs, this first-order transition path reduces the barrier to switching by more than 50% as compared to switching through the high-symmetry $P6_3/mmc$ structure, and makes it more likely that the material will return to the ground state when the external field is switched off.

We use maximally localized Wannier functions to analyze differences in bonding between the $P6_3mc$ and $Pnma$ structures and to study how the bonding changes when the material is switched. While we refer to the previously synthesized NaCdAs as our example, we find that our description of bonding is similar in other combinations. The bonding orbitals of the $P6_3mc$ structure are sp^3-like orbitals centered near As, the most electronegative element, with all bonds oriented towards the

four neighboring Cd atoms (see Fig. 2). The bonds of the $Pnma$ structure are also sp^3-like and centered on As; however, a transition between the two structures requires that half of the sp^3 bonds reorient. This proceeds by breaking an inter-layer Cd-As bond, with this orbital forming a p_z-like non-bonding state in the transition structure, and then reforming the bond pointing in the other direction (see the orbital in Fig. 2). In addition, the in-plane sp^3 bonds reorient by passing through an sp^2-like intermediate state. The similar bonding in the $P6_3mc$ and $Pnma$ structures is consistent with their competitive energies. However, we note that in the $Pnma$ structure, only half of the sp^3 bonds are oriented directly between Cd and As, which accounts for the significant changes in band gap between the two structure types.

Our proposed antiferroelectrics have many properties that could make them better for applications than existing materials. For instance, most of our candidates have a change in volume of 1-4 % upon switching (see Table I), which is much larger than the change observed in most piezoelectrics (0.1-0.2 %) and current antiferroelectrics (≤ 0.9 %) [11]. Very large volume changes could make these materials ideal for a variety of transducer applications in which harnessing a large non-linear response is necessary. Another application would be to use these antiferroelectrics as a substrate which could apply a reversible strain to thin films grown on top. We also note that in contrast to perovskite oxides, the stability of the polar and antipolar distortions in these materials is relatively insensitive to strain [5], these materials have no competing distortion patterns, and they are strongly anisotropic, a combination of favorable properties which could make antiferroelectric ABC useful in applications that require a robust and reversible response to external fields, such as high-energy storage capacitance and electrocaloric refrigeration.

In conclusion, we have used first-principles methods to establish a new class of antiferroelectrics in the MgSrSi structure type and to identify promising candidate materials for further investigation. Through targeted synthesis, MgSrSi-type compounds could potentially be developed as a valuable class of functional antiferroelectric materials. This is a specific application of a larger-scale strategy to identify new functional materials by targeting insulating compounds not previously recognized as functional materials and tuning the composition and other control parameters, such as epitaxial strain, and/or modifying the structure by intercalation of atoms. The identification of antiferroelectricity in classes of materials in which it was previously unrecognized offers the possibility of optimizing properties and combining polarization with other functional properties, including magnetism, to produce multifunctional behavior of fundamental scientific interest and for groundbreaking technological applications.

————

[1] A. Jain, G. Hautier, C. J. Moore, S. P. Ong, C. C. Fischer, T. Mueller, K. A. Persson, and G. Ceder, Comp. Mater. Science **50**, 2295 (2011).

[2] R. Armiento, B. Kozinsky, M. Fornari, and G. Ceder, Phys. Rev. B **84**, 014103 (2011).

[3] X. Zhang, L. Yu, A. Zakutayev, and A. Zunger, Adv. Funct. Mater. **22**, 1425 (2012).

[4] A. Roy, J. W. Bennett, K. M. Rabe, and D. Vanderbilt, Phys. Rev. Lett. **109**, 037602 (2012).

[5] J. W. Bennett, K. F. Garrity, K. M. Rabe, and D. Vanderbilt, Phys. Rev. Lett. **109**, 167602 (2012).

[6] J. W. Bennett and K. M. Rabe, J. Solid State Chem. **195**, 21 (2012).

[7] M. E. Lines and A. M. Glass, *Principles and Applications of Ferroelectrics and Related Materials* (Clarendon Press, Oxford, 1977).

[8] S. Ogale and V. Venkateshan, eds., *Functional Metal Oxides: New Science and Novel Applications* (Wiley, 2012).

[9] G. Shirane, E. Sawaguchi, and Y. Takagi, Phys. Rev. **84**, 476 (1951).

[10] C. Kittel, Phys. Rev. **82**, 729 (1951).

[11] Y. Yu, J. Tu, and R. J. Singh, J. Am. Ceram. Soc. **84**, 333 (2001).

[12] A. S. Mischenko, Q. Zhang, J. F. Scott, R. W. Whatmore, and N. D. Mathur, Science **311**, 1270 (2006).

[13] B. Jaffe, Proc. of the IRE pp. 1264–1267 (1961).

[14] X. Tan, C. Ma, J. Frederick, S. Beckman, and K. G. Webber, J. Am. Ceram. Soc. **94**, 4091 (2011).

[15] H. Fujishita, Y. Shiozaki, N. Achiwa, and E. Sawaguchi, J. Phys. Soc. Jpn. **51**, 3583 (1982).

[16] S. K. Mishra, N. Choudhury, S. L. Chaplot, P. S. R. Krishna, and R. Mittal, Phys. Rev. B **76**, 024110 (2007).

[17] I. Jankowska-Sumara, Phys. Stat. Sol. **244**, 1887 (2007).

[18] D. Kan, L. Palova, V. Anbusathaiah, C. J. Cheng, S. Fujino, V. Nagarajan, K. M. Rabe, and I. Takeuchi, Adv. Funct. Mat. **20**, 1108 (2010).

[19] D. H. Kim, H. N. Lee, M. Varela, and H. M. Christen, Appl. Phys. Lett. **89**, 162904 (2006).

[20] R. Blinc and B. Zeks, eds., *Soft modes in ferroelectrics and antiferroelectrics* (North-Holland, 1974).

[21] B. Eisenmann, H. Schaefer, and A. Weiss, Zeit.fuer Anorg. All. Chem. **391**, 241 (1972).

[22] C. B. Shoemaker and D. P. Shoemaker, Acta Cryst. **18**, 900 (1965).

[23] S. Liu and J. D. Corbett, J. Solid State Chem. **179**, 830 (2006).

[24] Y. Katsura and H. Takagi, J. Electronic Mater. (2012).

[25] J. W. Bennett, I. Grinberg, and A. M. Rappe, J. Am. Chem. Soc. **130**, 17409 (2008).

[26] J. W. Bennett, I. Grinberg, P. K. Davies, and A. M. Rappe, Phys. Rev. B **82**, 184106 (2010).

[27] G. Y. Gou, J. W. Bennett, H. Takenaka, and A. M. Rappe, Phys. Rev. B **83**, 205115 (2011).

[28] X. Gonze, B. Amadon, P. Anglade, J. M. Beuken, F. Bottin, P. Boulanger, F. Bruneval, D. Caliste, R. Caracas, M. Cote, et al., Comp. Phys. Comm. **180**, 2582 (2009).

[29] H. J. Monkhorst and J. D. Pack, Phys. Rev. B **13**, 5188 (1976).

[30] R. D. King-Smith and D. Vanderbilt, Phys. Rev. B **47**, 1651 (1993).

[31] R. Resta, Rev. Mod. Phys. **66**, 899 (1994).

[32] A. M. Rappe, K. M. Rabe, E. Kaxiras, and J. D. Joannopoulos, Phys. Rev. B Rapid Comm. **41**, 1227 (1990).

[33] N. J. Ramer and A. M. Rappe, Phys. Rev. B **59**, 12471 (1999).

[34] http://opium.sourceforge.net.

[35] P. Giannozzi and et al., J. Phys.:Condens. Matter **21**, 395502 (2009).

[36] H. Jonsson, G. Mills, and K. W. Jacobsen, in *Classical and Quantum Dynamics in Condensed Phase Simulations*, edited by B. J. Berne, G. Ciccotti, and D. F. Coker (World Scientific, 1998), p. 385.

[37] G. Henkelman, B. P. Uberuaga, and H. Jonsson, J. Phys. Chem. **113** (2000).

[38] A. A. Mostofi, J. R. Yates, Y.-S. Lee, I. Souza, D. Vanderbilt, and N. Marzari, Comput. Phys. Commun. **178**, 685 (2008).

[39] N. Marzari and D. Vanderbilt, Phys. Rev. B **56**, 12847 (1997).

[40] A. Belsky, M. Hellenbrandt, V. L. Karen, and P. Luksch, Acta Cryst. **B58**, 364 (2002).

[41] G. B. Bachelet and N. E. Christensen, Phys. Rev. B **31**, 879 (1985).

[42] K. Schwarz and P. Blaha, Comp. Mater. Sci. **28**, 259 (2003).

[43] J. W. Bennett, Physics Procedia **30**, 14 (2012).

[44] For select combinations in which the error in lattice constant is larger, on the order of 3-4%, we perform all-electron calculations as implemented in Wien2K [42], and obtain lattice constants similar to those predicted (Supplemental Materials) using the Bennett-Rappe library of pseudopotentials (design parameters described in Ref. [43]).

[45] We believe that these few discrepancies, as well as those combinations in which only one refinement was present in the ICSD, warrant further experimental investigations.